

Optimization of monolithic silica aerogel insulants

J. FRICKE, X. LU, P. WANG, D. BÜTTNER and U. HEINEMANN

Physikalisches Institut der Universität, Am Hubland, D-8700 Würzburg, F.R.G.

(Received 18 April 1991)

Abstract—In this work we systematically investigate thermal transport in opacified monolithic silica aerogels by changing their density and the concentration of infrared opacifier. The goal is to minimize the thermal conductivity of these highly porous inorganic materials. The lowest achieved thermal conductivities at 300 K are about $0.013 \text{ W m}^{-1} \text{ K}^{-1}$ for non-evacuated specimens, which have to be compared with values of about $0.020\text{--}0.025 \text{ W m}^{-1} \text{ K}^{-1}$ for CFC-blown insulating polyurethane foams and with $0.035 \text{ W m}^{-1} \text{ K}^{-1}$ for the best fiber insulations. Our investigations allow us to quantitatively determine the gaseous, solid and radiative conductivities λ_g , λ_s and λ_r , respectively. The derived variations with aerogel density ρ are: $\lambda_g \propto \rho^{-0.6}$, $\lambda_s \propto \rho^{1.5}$ and $\lambda_r \propto (\rho \cdot e)^{-1}$ in the range $70 < \rho/\text{kg m}^{-3} < 230$. The total conductivity shows a minimum around 120 kg m^{-3} .

1. INTRODUCTION

SILICA aerogel [1–3] is a highly porous material made in a sol-gel process with subsequent supercritical drying. Transparent aerogels in monolithic or granular form are valuable materials for passive solar usage [4] and thus for energy conservation. Silica aerogels are known for their high optical transparency [5] as well as their excellent thermal insulation [6] at ambient temperatures. Today, monolithic aerogel tiles of sizes up to $40 \times 40 \times 2 \text{ cm}^3$ [7] are available in small quantities. Granular aerogel is more easily and cheaply produced [8]. We have demonstrated that aerogels can also serve as efficient opaque insulations in refrigerators, freezers and heat storage systems [9]. For this application the gel has to be opacified with TiO_2 , iron oxide or carbon soot. Silica aerogel powder is most attractive as an insulant, as it can be easily filled into hollow spaces. In air, this material has a surprisingly low conductivity of about $0.020 \text{ W m}^{-1} \text{ K}^{-1}$ at 300 K [9]. It can thus be considered a non-flammable, non-toxic and environmentally favorable substitute for CFC-blown polyurethane foam. Evacuated, load bearing aerogel powder has a thermal conductivity of only about $0.004 \text{ W m}^{-1} \text{ K}^{-1}$. It can thus compete with fibrous superinsulations from a conductivity point of view [10]; the handling of aerogel powder is much easier and does not cause the health problems apprehended for fiber systems.

A prerequisite for the further improvement of aerogel powders is the optimization of the thermal resistance of monolithic aerogels. This goal was pursued in our laboratory; the results are presented in this paper.

2. DESCRIPTION OF HEAT TRANSFER

The addition of an infrared (i.r.) opacifier is important for the reduction of radiative heat transfer in

silica aerogels, which show low infrared absorption in the $3\text{--}8 \mu\text{m}$ spectral region [11]. In addition, opacification makes data interpretation much easier, as the radiative conductivity is linearly superimposed on the gaseous and solid conductivity in this case, while complex coupling phenomena occur for pure SiO_2 aerogels [11].

2.1. Radiative transport

Pure silica is an effective i.r. absorber for wavelengths above $8 \mu\text{m}$ (Fig. 1). The specific extinction here is $e \geq 100 \text{ m}^2 \text{ kg}^{-1}$ [9]. Below $8 \mu\text{m}$ the absorption, however, is extremely small. An improved i.r. extinction in this range can be provided by the addition of opacifiers with strong i.r. absorption, e.g. soot, or efficient scattering, e.g. titania.

If optically thick media are considered, the temperature dependence of the radiative conductivity is

$$\lambda_r = (16/3)n^2\sigma T_r^3/[e(T_r) \cdot \rho]. \quad (1)$$

The product $e \cdot \rho = E$ is the extinction coefficient,

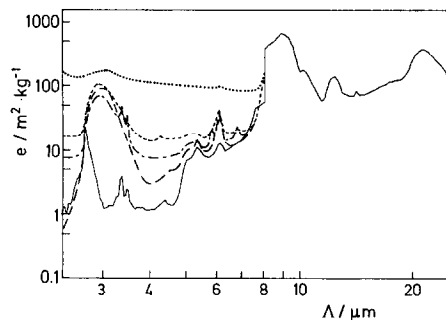


FIG. 1. Spectral specific extinction $e(\lambda)$ of pure and opacified SiO_2 aerogel. (—) Pure SiO_2 aerogel, baked; (---) pure SiO_2 aerogel; (-·-·-) aerogel plus 0.1% soot; (---) 0.5% soot; (····) 5% soot.

NOMENCLATURE

e	mass specific extinction	γ	scaling exponent
E	extinction coefficient	δ	scaling exponent
g	ratio between solid conductivities of vitreous silica and aerogel	λ	thermal conductivity
Kn	Knudsen number	Λ	wavelength
l	mean free path	ρ	density
n	index of refraction	σ	Stefan-Boltzmann constant
p	gas pressure	ϕ	diameter of pores or particles.
T	temperature.		
Greek symbols		Subscripts	
α	scaling exponent	g	gaseous
β	dimensionless parameter in Knudsen's formula	r	radiative
		s	solid.

which is equal to $1/l_{\text{photon}}$, with l_{photon} the photon mean free path. In optically thick insulations the photon mean free path is very small compared to the thickness of the specimen. The specific extinction coefficient $e(T_r)$ is derived from the spectral specific extinction $e(\Lambda)$ by proper spectral averaging (Rosseland mean). n is the mean index of refraction of the insulation; for low-density insulations n is close to 1. σ is the Stefan-Boltzmann constant. T_r is the radiative temperature calculated from the boundary temperatures T_1 and T_2

$$T_r^3 = (1/4) \cdot (T_1^2 + T_2^2) \cdot (T_1 + T_2). \quad (2)$$

From equation (1) we learn that the radiative contributions are smaller, the larger the extinction coefficient E is. An effective diminution of λ_r is thus expected from an increase of both density ρ and specific extinction e . The latter can be realized by increasing the amount of opacifier integrated into the aerogel skeleton. The optimal distribution of the opacifier is important in this respect.

The achieved specific extinction of a pure and an opacified aerogel as a function of temperature is shown in Fig. 2. The data were calculated from the spectral measurements, which were performed with platelets less than 1 mm thick. For aerogels of density $\rho \approx 100 \text{ kg m}^{-3}$ with 5% carbon soot one thus expects

a specific extinction of around $100 \text{ m}^2 \text{ kg}^{-1}$. As we shall see later, such high extinction values are not achieved in larger specimens necessary for calorimetric measurements. Possibly the opacifier, which was added to the chemical solution prior to gelation, had agglomerated, thus lowering the specific extinction.

2.2. Solid conduction

The solid conductivity λ_s of SiO_2 aerogels is considerably smaller than the one for non-porous vitreous silica. Above about 50 K the variation of λ_s with temperature is the same as for vitreous silica [12]. The absolute amount of the conductivities can be described by a geometric factor (Fig. 3), $g = \lambda_s(\text{vitreous silica})/\lambda_s(\text{aerogel})$.

For low density aerogels with $\rho \approx 100 \text{ kg m}^{-3}$ the factor g is typically of the order of several hundred. Between $\rho = 70$ and 300 kg m^{-3} a variation

$$\lambda_s \propto \rho^\alpha, \quad \text{with } \alpha \approx 1.5 \quad (3)$$

can be found. This agrees well with earlier predictions [13, 14].

2.3. Gaseous conduction

Monolithic aerogels have pores in the 1–100 nm size regime. According to Knudsen's equation the gaseous conductivity λ_g within these pores varies with

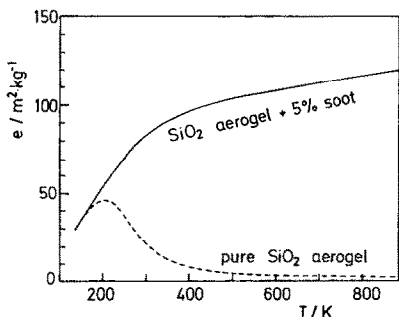


FIG. 2. Rosseland mean of specific extinction e of pure and opacified monolithic aerogels vs temperature.

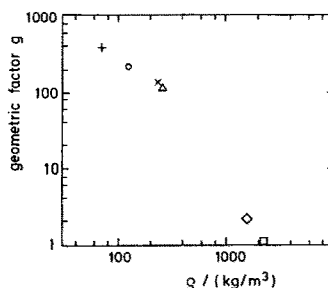


FIG. 3. Geometric factor $g = \lambda_s(\text{vitreous silica})/\lambda_s(\text{aerogel})$ as a function of density ρ [12]. (+) Aerogel, 71 kg m^{-3} ; (O) 124 kg m^{-3} ; (x) 235 kg m^{-3} ; (Δ) 262 kg m^{-3} ; (\diamond) Vycor; (\square) vitreous silica.

$$\lambda_g = \frac{\lambda_{g0}}{1 + \beta \cdot Kn}. \quad (4)$$

λ_{g0} is the gaseous conductivity of a free gas and $\beta \approx 2$ for air. The Knudsen number is

$$Kn = l_g / \phi, \quad (5)$$

where l_g describes the mean free path of the gas particles and ϕ is an effective pore diameter. As Kn is of the order of 1 for aerogels at 300 K and $p_g = 1$ bar ($l_g \approx 70$ nm), the gaseous conductivity λ_g remains considerably below the value λ_{g0} . As a rule of thumb $\lambda_g < 0.01 \text{ W m}^{-1} \text{ K}^{-1}$ at 1 bar is observed.

Upon variation of aerogel density one expects a change of effective pore diameter:

$$\phi \approx (2/3)(\rho_0/\rho)\phi_0 \propto \rho^{-1}, \quad (6)$$

with $\rho_0 =$ density and $\phi_0 =$ diameter of aerogel subunits. Here a random distribution of subunits is assumed. For a more regularly built network, $\phi \propto \rho^{-\gamma}$, with $1/2 < \gamma < 1$, is valid.

After insertion of equation (6) into the above equations we get

$$\lambda_g = \lambda_{g0} \left\{ 1 + \rho \frac{3\beta l_g}{2\rho_0 \phi_0} \right\}^{-1}. \quad (7)$$

Thus λ_g is expected to decrease with increasing aerogel density.

2.4. Total conductivity

All three contributions to the heat transfer described above are superimposed linearly; thus the total conductivity of air-filled monolithic aerogels becomes

$$\lambda = \lambda_s + \lambda_r + \lambda_g \approx \lambda_{\text{evac}} + \lambda_g. \quad (8)$$

λ_{evac} is the conductivity of an evacuated aerogel specimen.

3. SAMPLE PREPARATION AND EXPERIMENTAL METHODS

A Pt hot wire probe was mounted in a glass tube, which was then filled with a mixture of TMOS, CH_3OH , water and finely dispersed carbon soot. A silica gel was formed under basic conditions, generally within 5 min. Supercritical drying in an autoclave was performed with respect to methanol. The density of the resulting aerogel cylinder was controlled by the TMOS- CH_3OH ratio, which is about 1:3 for a 100 kg m^{-3} aerogel. In crack-free specimens the Pt wires were rigidly connected to the aerogel body; thus a good thermal contact was guaranteed, even under evacuation.

The thermal conductivity was determined by feeding a constant electric power into the filament and by observation of its temperature increase [15].

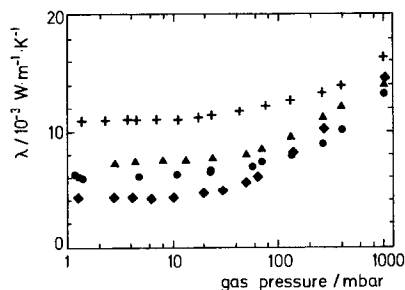


FIG. 4. Thermal conductivity λ of various monolithic aerogels at $T = 300$ K as a function of air pressure p_g . (+) $\rho = 230 \text{ kg m}^{-3}$, 2.5% soot; (▲) $\rho = 150 \text{ kg m}^{-3}$, 10% soot; (●) $\rho = 120 \text{ kg m}^{-3}$, 5% soot; (◆) $\rho = 75 \text{ kg m}^{-3}$, 5% soot.

4. RESULTS

The conductivity λ of monolithic aerogels with densities $\rho = 230, 150$ and 120 and 75 kg m^{-3} was determined for 300 K as a function of air pressure (Fig. 4). At $p_g = 1$ bar we found $\lambda \approx 0.017, 0.014, 0.013$ and $0.016 \text{ W m}^{-1} \text{ K}^{-1}$ for the four aerogels. To our knowledge, $0.013 \text{ W m}^{-1} \text{ K}^{-1}$ is the smallest conductivity ever reported for a non-evacuated solid body at 300 K. Whether this value is already the minimal conductivity achievable with opacified aerogels is currently being investigated.

Already at $p_g = 10\text{--}50$ mbar the gaseous conduction becomes negligible; the corresponding conductivity values at 300 K are $\lambda_{\text{evac}} \approx 0.011, 0.008, 0.006$ and $0.005 \text{ W m}^{-1} \text{ K}^{-1}$. We want to point out that pressures of 50 mbar are easy to obtain and maintain in evacuated insulation systems.

The variation of λ_{evac} of various evacuated monolithic aerogels with temperature is shown in Fig. 5. From the intersection of the fit line with the approximate ordinate values, the solid conductivity λ_s can be derived. These are found to be around 0.009, 0.004, 0.003 and $0.002 \text{ W m}^{-1} \text{ K}^{-1}$ for the four aerogels. From the slopes in Fig. 5 the specific extinction for the opacified aerogels can be estimated: $e = 15, 43, 40$ and $60 \text{ m}^2 \text{ kg}^{-1}$ result for the four specimens. As indicated above, these values are considerably below the spectroscopically derived data from thin samples.

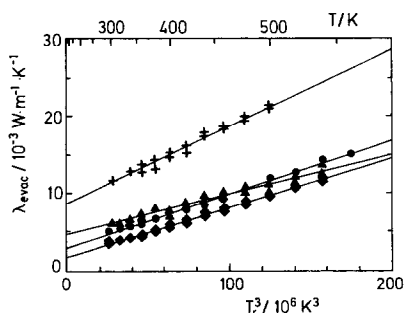


FIG. 5. Thermal conductivity λ_{evac} of various evacuated opacified monolithic SiO_2 aerogels vs T^3 . (+) $\rho = 230 \text{ kg m}^{-3}$, 2.5% soot; (▲) $\rho = 150 \text{ kg m}^{-3}$, 10% soot; (●) $\rho = 120 \text{ kg m}^{-3}$, 5% soot; (◆) $\rho = 75 \text{ kg m}^{-3}$, 5% soot.

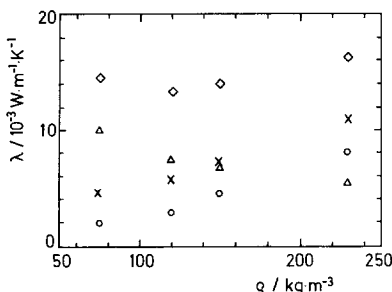


FIG. 6. Total conductivity for non-evacuated and evacuated aerogel, λ (\diamond) and λ_{vac} (\times), respectively, as well as gaseous and solid conductivity, λ_g (\triangle) and λ_s (\circ), respectively, as a function of density ρ .

5. DISCUSSION

The total conductivities before and after evacuation, λ and λ_{vac} , respectively, for four different aerogel densities at $T \approx 300$ K are shown in Fig. 6. The difference $\lambda - \lambda_{\text{vac}}$ equals the gaseous conductivity λ_g . The radiative conductivities λ_r are derived from the slopes in Fig. 5. If these values are subtracted from λ_{vac} , λ_s is finally obtained.

As anticipated, λ_r and λ_g decrease with increasing ρ , while λ_s increases. The experimentally derived dependences can be approximated by (see Fig. 7)

$$\lambda_g \propto \rho^{-\delta}, \quad \text{with } \delta \approx 0.6$$

$$\lambda_s \propto \rho^\alpha, \quad \text{with } \alpha \approx 1.5.$$

6. OUTLOOK

We have shown that the total conductivity λ as a function of aerogel density ρ displays a minimum with $\lambda = 0.013$ W m⁻¹ K⁻¹ at $\rho = 120$ kg m⁻³. A slight further decrease of λ seems possible, if the specific extinction e can be improved by a better distribution of the opacifier. However, we want to emphasize that

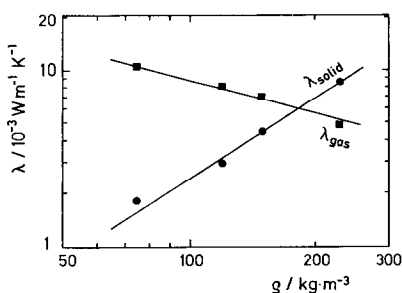


FIG. 7. Logarithm of λ_s and λ_g vs logarithm of aerogel density ρ . From the slopes scaling exponents $\alpha \approx 1.5$ and $\delta = -0.6$ can be derived.

the extremely small conductivities achieved up to now are not reached by other insulation systems in air.

The data for λ_s shown in Fig. 6 are somewhat higher than those used for Fig. 3. This may be due to inaccuracies of the caloric measurements (which we estimate to be ± 0.001 W m⁻¹ K⁻¹) and the fact that the aerogels were grown under different conditions. It would be worthwhile concentrating on the comparison of differently grown aerogels in future caloric investigations.

REFERENCES

1. J. Fricke (Editor), *Aerogels*, Springer Proceedings in Physics, Vol. 6. Springer, Berlin (1985).
2. R. Vacher, J. Phalippou, J. Pelous and T. Woignier (Editors), *Revue de Physique Appliquée*, Coll. C4, Suppl. 4. Les editions de Physique, Les Ulis (1989).
3. J. Fricke and A. Emmerling, Aerogels—Preparation, properties, applications. In *Chemistry, Spectroscopy and Applications of Sol-Gel Glasses* (Edited by R. Reisfeld and C. K. Jørgensen), Springer Series, Structure and Bonding, Vol. 77. Springer, Berlin (1992).
4. A. Goetzberger and A. Wittwer, Translucent insulation for passive solar energy utilization in buildings. In *Aerogels*, Springer Proceedings in Physics, Vol. 6, pp. 84–93. Springer, Berlin (1985).
5. P. H. Tewari, A. J. Hunt and K. D. Lofftus, Advances in production of transparent silica aerogels. In *Aerogels*, Springer Proceedings in Physics, Vol. 6, pp. 31–37. Springer, Berlin (1985).
6. D. Büttner, R. Caps, U. Heinemann, E. Hümmer, A. Kadur, P. Scheuerpflug and J. Fricke, Thermal conductivity of SiO₂-aerogel tiles. In *Aerogels*, Springer Proceedings in Physics, Vol. 6, pp. 104–109. Springer, Berlin (1985).
7. S. Henning, Airglass, Staffanstorp (Sweden), private communication.
8. I. J. Broecker, W. Heckmann, F. Fischer, M. Mielke, J. Schroeder and A. Stange, Structural analysis of granular silica aerogels. In *Aerogels*, Springer Proceedings in Physics, Vol. 6, pp. 160–166. Springer, Berlin (1985).
9. J. Fricke, M. C. Arduini-Schuster, D. Büttner, H.-P. Ebert, U. Heinemann, J. Heffleisch, E. Hümmer, J. Kuhn and X. Lu, Opaque silica aerogel insulations as substitutes of polyurethane (PU) foams, *21st Int. Thermal Conductivity Conf.*, Lexington, KY (Oct. 1989).
10. D. Büttner, J. Fricke and H. Reiss, Thermal conductivity of evacuated load-bearing powder and fiber insulations under variable external load, *High Temp.-High Pressures* **17**, 333–341 (1985).
11. P. Scheuerpflug, R. Caps, D. Büttner and J. Fricke, Apparent thermal conductivity of evacuated SiO₂-aerogel tiles under variation of radiative boundary conditions, *Int. J. Heat Mass Transfer* **28**, 2299–2306 (1985).
12. P. Scheuerpflug, H.-J. Morper, G. Neubert and J. Fricke, Low temperature thermal transport in silica aerogels, *J. Phys. D: Appl. Phys.* **24**, 1395–1403 (1991).
13. O. Nilsson, Å. Fransson and O. Sandberg, Thermal properties of silica aerogels. In *Aerogels*, Springer Proceedings in Physics, Vol. 6, pp. 121–126. Springer, Berlin (1985).
14. J. Fricke, R. Caps, D. Büttner, U. Heinemann and E. Hümmer, Silica-aerogel—a light transmitting thermal superinsulator, *J. Non-Cryst. Solids* **95/96**, 1167–1174 (1987).
15. H. S. Carslaw and J. C. Jaeger, *Conduction of Heat in Solids*, 2nd Edn. Oxford University Press, London (1959).

OPTIMISATION DES SILICA-AEROSOLS MONOLITHES ISOLANTS

Résumé—On étudie systématiquement le transfert thermique dans des silica-aérosols monolithes opacifiés en changeant leur densité et la concentration de l'opacifiant d'infrarouge. Le but est de diminuer la conductivité thermique de ces matériaux inorganiques fortement poreux. Les plus faibles conductivités thermiques obtenues à 300 K sont proches de $0,013 \text{ W m}^{-1} \text{ K}^{-1}$ pour des spécimens non évacués, valeur à comparer avec celles comprises entre $0,02$ et $0,025 \text{ W m}^{-1} \text{ K}^{-1}$ pour les mousses de polyuréthane soufflées aux CFC et avec $0,035 \text{ W m}^{-1} \text{ K}^{-1}$ pour les meilleurs isolants fibreux. Cette étude permet de déterminer quantitativement les conductivités thermiques de conduction dans le gaz et le solide et de rayonnement, respectivement λ_g , λ_s et λ_r . Leurs variations avec la masse volumique de l'aérosol sont : $\lambda_g \propto \rho^{-0,6}$, $\lambda_s \propto \rho^{1,5}$ et $\lambda_r \propto (\rho \cdot e)^{-1}$ dans le domaine $70 < \rho/\text{kg m}^{-3} < 230$. La conductivité totale est minimale vers 120 kg m^{-3} .

OPTIMIERUNG VON WÄRMEDÄMMUNGEN AUS INFRAROT-GETRÜBTE AEROGELN

Zusammenfassung—Im Rahmen dieser Arbeit wurde der Wärmetransport in infrarot-getrübten Aerogelen als Funktion der Dichte und Konzentration des Trübungsmittels systematisch untersucht. Zielsetzung war die Minimierung der Wärmeleitfähigkeit solcher hochporöser anorganischer Materialien. Die bisher geringste Wärmeleitfähigkeit im belüfteten Zustand bei 300 K war etwa $0,013 \text{ W m}^{-1} \text{ K}^{-1}$ —dies muß mit Werten von $0,020$ bis $0,025 \text{ W m}^{-1} \text{ K}^{-1}$ für FCKW-geblähte PU-Schäume und $0,035 \text{ W m}^{-1} \text{ K}^{-1}$ für die besten Faserdämmaterialien verglichen werden. Unsere Untersuchungen erlauben die quantitative Bestimmung von Gas-, Festkörper- und Strahlungswärmeleitfähigkeit λ_g , λ_s bzw. λ_r . Es zeigt sich, daß diese Größen mit der Aerogeldichte im Dichtebereich von $70 < \rho/\text{kg m}^{-3} < 230$ wie folgt variieren : $\lambda_g \propto \rho^{-0,6}$, $\lambda_s \propto \rho^{1,5}$ sowie $\lambda_r \propto (\rho \cdot e)^{-1}$. Die Gesamtwärmeleitfähigkeit zeigt bei einer Dichte von ca. 120 kg m^{-3} ein Minimum.

УЛУЧШЕНИЕ СВОЙСТВ МОНОЛИТНЫХ ИЗОЛЯЦИЙ ИЗ КРЕМНЕЗЕМНОГО АЭРОГЕЛЯ

Аннотация—Исследуется теплоперенос в замутненных кремнеземных аэрогелях посредством изменения их плотности и концентрации замутняющего вещества. Целью исследования являются минимизация теплопроводности используемых высокопористых неорганических веществ. Наиболее низкие коэффициенты теплопроводности были получены при 300 К для неоткаченных образцов и составляли примерно $0,013 \text{ Вт м}^{-1} \text{ К}^{-1}$, что отличается от значений, равных приблизительно $0,020$ – $0,025 \text{ Вт м}^{-1} \text{ К}^{-1}$, для изоляционных полиуретановых пен, продуваемых CFC, и от значения $0,035 \text{ Вт м}^{-1} \text{ К}^{-1}$ для лучших волокнистых изоляций. Количественно определены значения теплопроводности газа, твердой фазы и теплопроводности излучением λ_g , λ_s и λ_r . В интервале $70 < \rho/\text{кг м}^{-3} < 230$ получены следующие изменения плотности аэрогеля ρ : $\lambda_g \propto \rho^{-0,6}$, $\lambda_s \propto \rho^{1,5}$ и $\lambda_r \propto (\rho \cdot e)^{-1}$. Суммарная теплопроводность достигает минимума вблизи значения 120 кг м^{-3} .